# Biological Weighting Function for the Inhibition of Phytoplankton Photosynthesis by Ultraviolet Radiation

John J. Cullen,* Patrick J. Neale, Michael P. Lesser

Severe reduction of stratospheric ozone over Antarctica has focused increasing concern on the biological effects of ultraviolet-B (UVB) radiation (280 to 320 nanometers). Measurements of photosynthesis from an experimental system, in which phytoplankton are exposed to a broad range of irradiance treatments, are fit to an analytical model to provide the spectral biological weighting function that can be used to predict the short-term effects of ozone depletion on aquatic photosynthesis. Results show that UVA (320 to 400 nanometers) significantly inhibits the photosynthesis of a marine diatom and a dinoflagellate, and that the effects of UVB are even more severe. Application of the model suggests that the Antarctic ozone hole might reduce near-surface photosynthesis by 12 to 15 percent, but less so at depth. The experimental system makes possible routine estimation of spectral weightings for natural phytoplankton.

Declines in the concentration of stratospheric $O_3$ (*1*), particularly in the Antarctic during the austral spring (*2*), result in more UVB radiation reaching the earth's surface (*3*) and the upper part of aquatic photic zones (*4*, *5*). Environmental UVB is harmful to many biological processes (*6*–*9*), so intense efforts have been made to assess the photobiological effects of stratospheric $O_3$ depletion (*6*). Biological effects of absorbed ultraviolet radiation (UV) are generally a function of wavelength; therefore, they are best quantified with a spectral biological weighting function (*3*, *7*, *8*). The weighting function, comparable to an action spectrum (*7*, *9*), should accommodate interactions between (i) the UV that damages photosynthetic processes and (ii) longer wavelengths, which activate processes that counteract the damage (*4*, *10*). That is, photoinhibition is likely to be a function of both UV and the ratio between UV and photosynthetically active radiation (PAR, 400 to 700 nm) (*11*). A good model of spectral dependence is particularly important for studies of aquatic photosynthesis, because both UV and the ratio UV:PAR change with depth in the water column (*5*).

We constructed an analytical model of photosynthesis to describe the interaction

J. J. Cullen, Department of Oceanography, Dalhousie University, Halifax, Nova Scotia, Canada B3H 4J1, and Bigelow Laboratory for Ocean Sciences, McKown Point, West Boothbay Harbor, ME 04575.
P. J. Neale, Department of Plant Biology, University of California, Berkeley, CA 94720, and Bigelow Laboratory for Ocean Sciences, McKown Point, West Boothbay Harbor, ME 04575
M. P. Lesser, Bigelow Laboratory for Ocean Sciences, McKown Point, West Boothbay Harbor, ME 04575.
*To whom correspondence should be addressed

of UV and PAR in determining the rate of photosynthesis:

$$P^B = P_s^B(1 - e^{-E_{PAR}/E_s}) \left(\frac{1}{1 + E^*_{inh}}\right) \quad (1)$$

where $P^B$ (in grams of carbon per gram of chlorophyll per hour) is the rate of photosynthesis normalized to chlorophyll a, $P_s^B$ is the maximum attainable rate of photosynthesis in the absence of photoinhibition, $E_{PAR}$ is PAR expressed as irradiance (in watts per square meter), and $E_s$ is the saturation parameter for photosynthesis (*12*, *13*). As in other models, $P^B$ is the product of potential photosynthesis, $P_s^B[1 - \exp(-E_{PAR}/E_s)]$, and inhibition, $1/(1 + E^*_{inh})$. In this model, however, the inhibition term is a function of both UV irradiance ($E_{UV}$) and $E_{PAR}$ as expressed in the biologically weighted, dimensionless dose rate, $E^*_{inh}$,

$$E^*_{inh} = \bar{\epsilon}_{PAR}E_{PAR} + \sum_{\lambda=280\text{ nm}}^{400\text{ nm}} \epsilon(\lambda)E(\lambda)\Delta\lambda \quad (2)$$

where $\bar{\epsilon}_{PAR}$ (in reciprocal watts per square meter) is the relative biological efficiency for damage to photosynthesis by $E_{PAR}$, $\epsilon(\lambda)$ is the wavelength-dependent biological efficiency for damage to photosynthesis by UV (*5*, *7–9*, *11*), and $E(\lambda)$ is spectral irradiance (in watts per square meter per nanometer) (*14–16*). As required for describing the variation of the amount of UV photoinhibition with depth in the ocean, this model predicts $P^B$ versus $E_{PAR}$ as a function of biological dose rate per unit $E_{PAR}$ (*17*) (Fig. 1) and responds directly to depth-dependent changes in the $E_{UV}$:$E_{PAR}$ ratio.

The model provides an analytical context for estimating the biological parameters that determine photosynthetic rate: maximum photosynthetic potential, $P_s^B$; the saturation parameter, $E_s$; the sensitivity of photosynthetic systems to supersaturating $E_{PAR}$, $\bar{\epsilon}_{PAR}$; and the biological weighting function for inhibition of photosynthesis by UV, $\epsilon(\lambda)$ ($\lambda$ = 280 to 400 nm). The first three parameters are under physiological control (*13*, *18*, *19*), and their variability in nature has been described (*20*). However, very little is known about the biological weighting function for phytoplankton. We therefore developed a procedure for estimating the biological weighting function in Eq. 2 and using it in Eq. 1 to predict photosynthesis as a function of UV and PAR in nature, as influenced by $O_3$ depletion.

An experimental system (the photoinhibitron) was developed for measuring photosynthesis of phytoplankton suspensions during controlled, quantified exposures to a broad range of $E_{PAR}$ and $E_{UV}$:$E_{PAR}$ (*21*). An incubator, modeled after a device for measuring action spectra of photosynthesis (*22*), was designed to hold samples of 2 to 3 ml each in a temperature-controlled block (20° ± 1°C), exposed to $E_{UV}$ + $E_{PAR}$ from below. Irradiance was provided by a 1000-W xenon illuminator, reflected by a mirror upward through a heat trap of circulating water. Appropriate UV-transparent or UV-reflective materials were used. The illuminated region was divided into eight sections, 5 by 5 cm, holding Schott series WG long-pass filters (*7*), with nominal cutoffs at 280, 295, 305, 320, 335, 345, and 365 nm (Fig. 2A). A 400-nm long-pass filter was used as a control with essentially no UV. Each section contained nine positions, which could be modified for selected transmittance by insertion of neutral-density perforated nickel screen (Fig. 2B). Results of experiments on cultures of a marine dinoflagellate and a diatom, when plotted as $P^B/P_s^B$ versus $E_{PAR}$ for different $E_{UV}$:$E_{PAR}$ ratios (Fig. 3, A and B), were qualita-

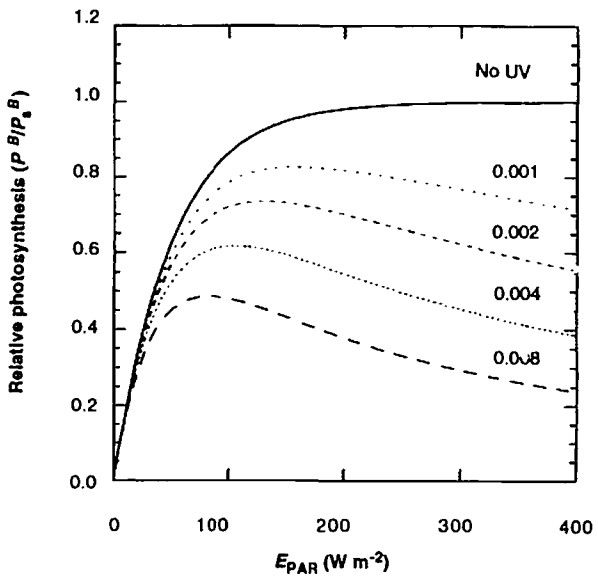


**Fig. 1.** Predictions of the analytical model of photosynthesis (Eq. 1): relative photosynthesis versus $E_{PAR}$ for different biological dose rates per unit $E_{PAR}$ [as labeled, see (*17*)]. In this example, there is no inhibition by $E_{PAR}$ alone ($\bar{\epsilon}_{PAR}$ = 0).

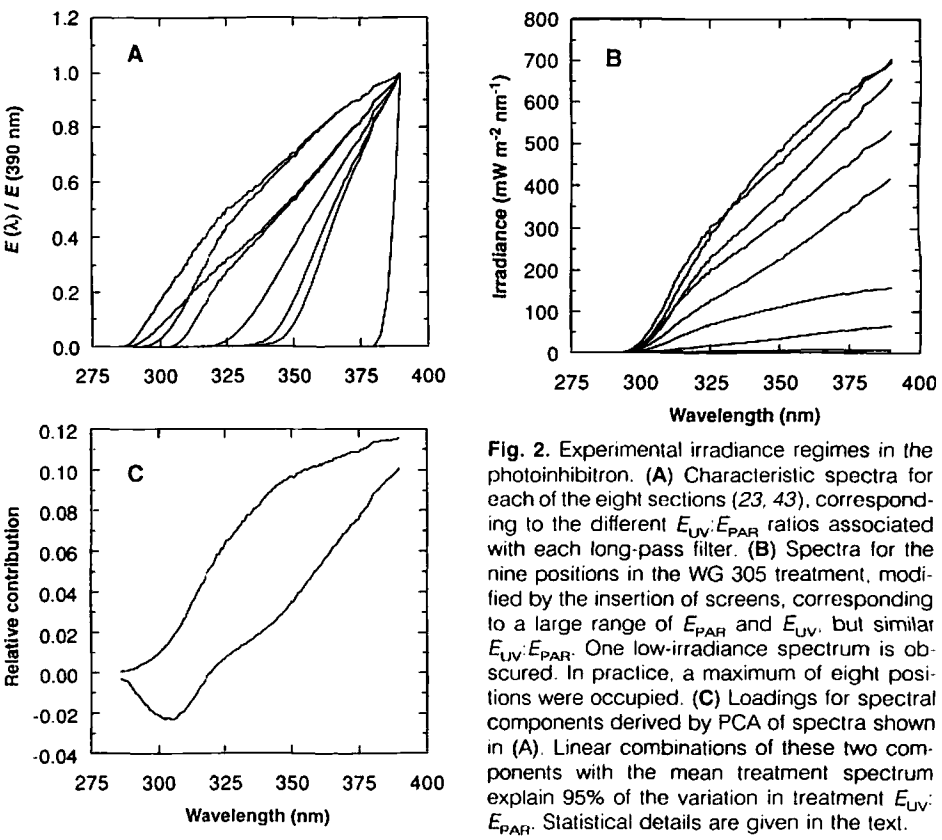


**Fig. 2.** Experimental irradiance regimes in the photoinhibitron. (**A**) Characteristic spectra for each of the eight sections (*23*, *43*), corresponding to the different $E_{UV}$:$E_{PAR}$ ratios associated with each long-pass filter. (**B**) Spectra for the nine positions in the WG 305 treatment, modified by the insertion of screens, corresponding to a large range of $E_{PAR}$ and $E_{UV}$, but similar $E_{UV}$:$E_{PAR}$. One low-irradiance spectrum is obscured. In practice, a maximum of eight positions were occupied. (**C**) Loadings for spectral components derived by PCA of spectra shown in (A). Linear combinations of these two components with the mean treatment spectrum explain 95% of the variation in treatment $E_{UV}$:$E_{PAR}$. Statistical details are given in the text.

tively consistent with the predictions of Eq. 1 and Fig. 1: the depression of $P^B$ at supersaturating intensities was exacerbated by exposure to shorter wavelengths.

Quantitative analysis of the experimental results required substitution (Eq. 2) for $E^*_{inh}$ in Eq. 1 and estimates of $P^B_s$, $E_o$, $\bar{\epsilon}_{PAR}$, and $\epsilon(\lambda)$ for UV wavelengths by nonlinear regression. The input consisted of ~100 measurements of $P^B$, $E_{PAR}$, and $E(\lambda)$ for $\lambda$ = 286 to 390 nm at 0.5-nm intervals (*23*). We simplified the analysis by applying multivariate statistical analysis to the spectra of $E_{UV}$ normalized to $E_{PAR}$. Briefly, we calculated a set of spectral components common to all UV treatments in an experiment using principal component analysis (PCA) (*24*). These sets of dimensionless spectral weightings were statistically defined so that any one UV treatment can be approximated by adding to or subtracting from the mean treatment spectrum a specific amount of each spectral component (the component "score"). More than 95% of the variance in UV treatment spectra could be represented with the first two components (Fig. 2C) (*25*). Instead of having to estimate directly the dependence of $E^*_{inh}$ on the UV spectral irradiance (Eq. 2), which would have required estimating a total of 209 coefficients [$\epsilon(\lambda)$, $\lambda$ = 286 to 390 nm at 0.5-nm intervals], we estimated the dependence of $E^*_{inh}$ on the two spectral component scores. This procedure required estimation of only three coefficients [$h_0$, the mean treatment effect over the whole irradiance spectrum including both $E_{PAR}$ and $E(\lambda)$, and the component effect, $h_i$, where $i$ corresponds to components 1, 2]. Then, the process was reversed: the coefficients $h_i$ were interpreted as the relative proportions of each spectral component required to generate a new spectral function describing the sensitivity of photosynthesis to UV, that is, the desired biological weighting function (*26*). This application of PCA is an efficient method for estimating simple, smoothly varying spectral responses without sacrificing spectral resolution and, unlike other methods (*7*), requires no a priori assumptions about spectral shape.

The PCA method was used to generate a biological weighting function for the photoinhibition of phytoplankton photosynthesis on the experimental time scale of 45 min (Fig. 3, C and D). The weighting functions from two different laboratory cultures were similar in shape, as would be expected if there was a general biological weighting function and if our analyses were robust. The dinoflagellate appeared to be somewhat more sensitive to UVB than the diatom, although the differences were not large (*27*). Normalized to 1.0 at 300 nm (Fig. 3E), our weighting function is similar to an action spectrum for photoinhibition of photosynthesis in the terrestrial plant, *Rumex patientia* (*7*). Our weighting function is also quite consistent with broad-band estimates of relative biological weighting for photoinhibition in natural Antarctic microalgae (*28*, *29*), at least between wavelengths of 312 and 355 nm.

In contrast to a previously determined weighting function for the inhibition of photosynthetic electron transport in vitro (*30*), our phytoplankton weighting function has a steep slope below 300 nm, like

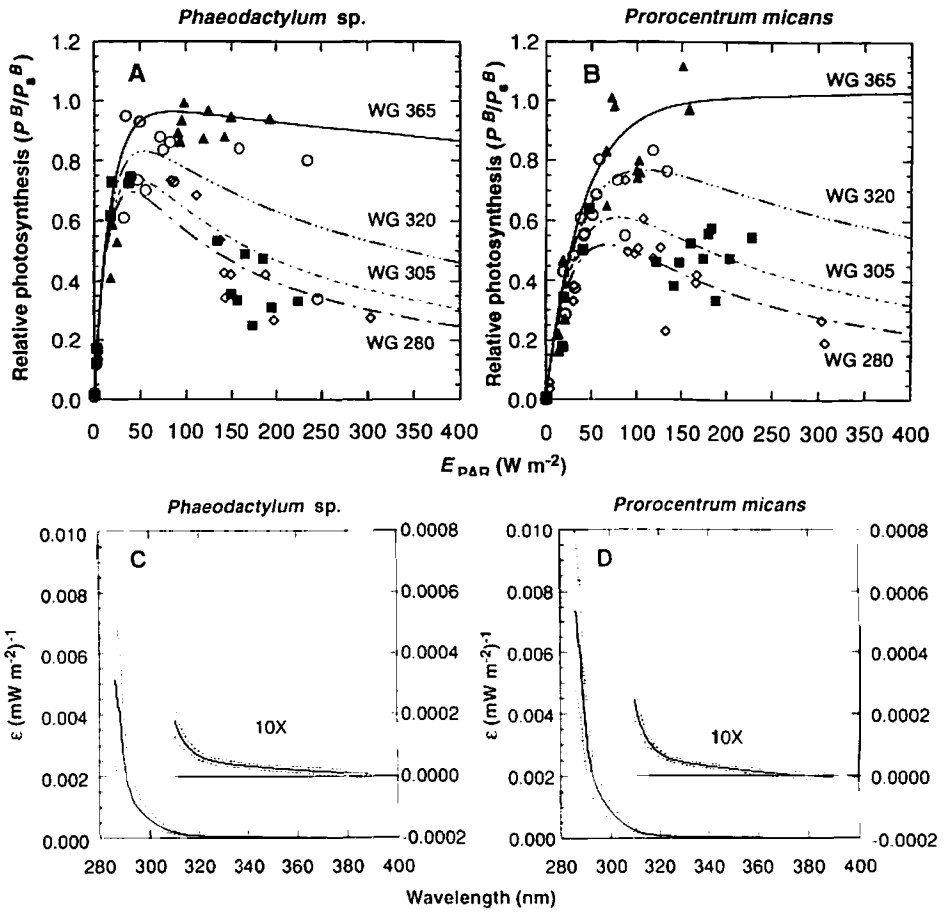


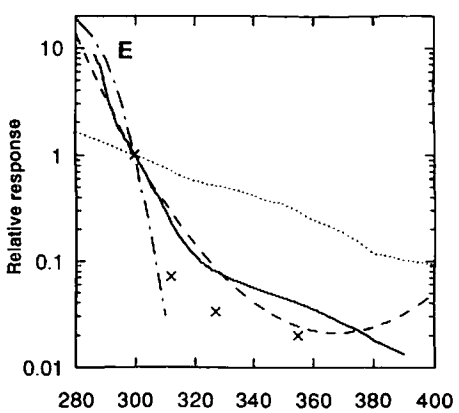


**Fig. 3.** Relative photosynthesis versus $E_{PAR}$ for phytoplankton exposed to different $E_{UV}$:$E_{PAR}$ ratios characteristic of each WG-series filter. For clarity, only four of the eight spectral treatments are shown: (**A**) *Phaeodactylum* sp., a diatom; (**B**) *Prorocentrum micans*, a dinoflagellate. The lines show a typical photosynthetic response for $P^B$ versus $E_{PAR}$ in each filter group when two spectral component scores ($c_1$,$c_2$) are substituted for UV irradiance in Eq. 1 (*24*–*26*). Spectral variation between cells in each treatment causes some of the scatter around these lines. In our model each cell is scored and fitted individually, and the total variance explained exceeds 93% for both fits. Symbols: WG 365 (▲), WG 320 (○), WG 305 (■), and WG 280 (◇). (**C** and **D**) Statistically determined biological weighting functions describing the experimental inhibition of photosynthesis by UV: *Phaeodactylum* sp. (C) and *Prorocentrum micans* (D). The solid line is the estimated weight and the dotted lines show the estimated 95% confidence interval of the estimate (*27*). Values for 310 to 390 nm are shifted, magnified, and repeated, with scaling on the right axis. (**E**) The weighting function for *Phaeodactylum* (——) compared to previously published action spectra, normalized to 1.0 at 300 nm: (· · ·) inhibition of photosynthetic electron transport in vitro (*30*) and (— · —) damage to DNA (*31*) as presented by Smith *et al.* (*8*); (· - · -) differential spectrum of inhibition of photosynthesis in the higher plant *Rumex patientia* (*7*); and (×) broad-band action spectrum estimates from experiments on inhibition of photosynthesis in Antarctic phytoplankton or sea-ice microalgae (*28*). The estimated 95% confidence interval for *Phaeodactylum* after normalization is approximately ±0.015 in the UVA spectral region.

that for damage to DNA (*31*) (Fig. 3E). Steeper slopes in the UVB range correspond to more severe predicted consequences of $O_3$ depletion (*7*). However, unlike the DNA function and more like inhibition of photosynthetic electron transport in vitro, our phytoplankton weighting function indicates a significant photoinhibitory effect well into the UVA; this is consistent with observations of photoinhibition in natural populations of phytoplankton (*4*, *28*, *29*, *32*). A significant response in the UVA, where natural irradiance greatly exceeds that in the UVB,

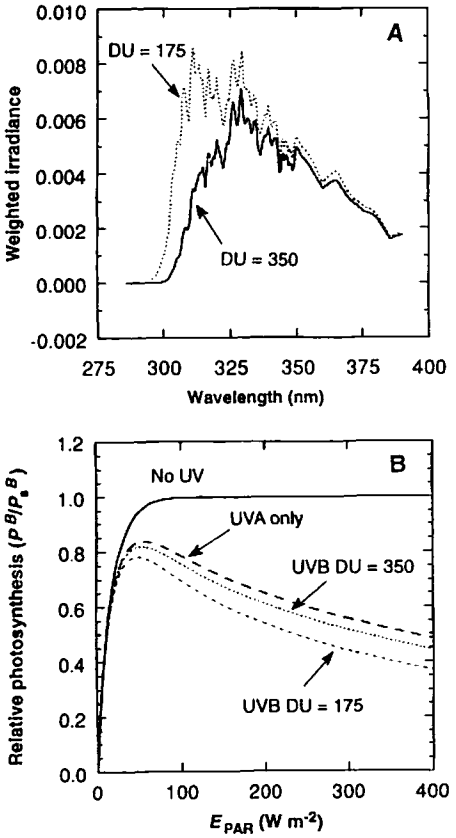


**Fig. 4.** (**A**) Biologically weighted UV dose rate [$\epsilon(\lambda)E(\lambda)\Delta\lambda$ at 0.5-nm intervals, dimensionless] in incident irradiance at local noon (0100 hours GMT) for McMurdo Station, Antarctica, on days of low atmospheric $O_3$ content [28 October 1990; Total Ozone Mapping System (TOMS) satellite estimate is ~175 Dobson units (1 DU = $10^{-3}$ cm)] and high atmospheric $O_3$ content (10 November 1990; TOMS is ~350 DU); spectra corresponding to 200 W m$^{-2}$ $E_{PAR}$ (*34*) were multiplied by the biological weighting coefficients estimated for *Phaeodactylum* sp. (Fig. 3C). (**B**) Trial calculation, using results from laboratory experiments on *Phaeodactylum* sp. (Fig. 3C) to predict photosynthesis versus $E_{PAR}$ under irradiance regimes in the Antarctic. The biological dose rate was calculated from spectra in (A) using dose rate per unit $E_{PAR}$ over 320 to 400 nm on 10 November 1990 (UVA only), over 286 to 400 nm on 10 November 1990 (UVB DU = 350) and over 286 to 400 nm on 28 October 1990 (UVB DU = 175).

tends to reduce predictions of the relative depression of photosynthesis associated with $O_3$ depletion (*6*, *7*).

In principle, our model can be used to assess the effects of $O_3$ depletion on aquatic primary production, with the use of direct measurements on natural populations of phytoplankton (*33*). We demonstrate the procedure with a trial calculation, based on measurements of incident spectral irradiance at McMurdo Station, Antarctica, as influenced by the $O_3$ hole (*34*), and the weighting function for a marine diatom grown in the laboratory (Fig. 4A). We consider the effects of UV on photosynthesis versus $E_{PAR}$ for high $O_3$ and low $O_3$ conditions (Fig. 4B).

The analysis predicts that damage from UVA dominates and produces about 40 to 50% inhibition of photosynthesis relative to that under $E_{PAR}$ alone, during exposures of 45 min to near-surface irradiance. Maximum midday $E_{PAR}$ recorded at McMurdo during November to December 1990 ranged from 225 to 340 W m$^{-2}$ (*34*). During high-$O_3$ conditions, UVB has only a small incremental effect; however, under low $O_3$ conditions, predicted photosynthetic rates were further reduced: 12 to 15% lower than under high $O_3$ conditions for $E_{PAR}$ characteristic of the sea surface in the Antarctic during the spring. The predicted effect of $O_3$ depletion is highly significant even given the inherent uncertainty in our estimates of the weighting coefficients; that is, a 12% relative decrease has an estimated 95% confidence interval of 10 to 15% (*35*). Because both $E_{PAR}$ and $E_{UV}$:$E_{PAR}$ decrease with depth (*4*, *5*), modeled relative inhibition associated with $O_3$ depletion would be much less for the water column as a whole than for the sea surface. For example, our model predicts that at 4 m, where PAR is 70% of the surface value, photosynthetic rates are incrementally reduced by only 6 to 7% during low $O_3$ conditions, assuming incident irradiance from McMurdo and relative spectral attenuation as reported for the Bellingshausen Sea (*4*). Our prediction depends on the heuristic assumption that the laboratory-derived biological weighting function for photoinhibition of photosynthesis applies for phytoplankton grown in the Antarctic under entirely different conditions. However, only the spectral shape of the weighting function need be conserved for the estimate of relative inhibition associated with $O_3$ depletion to be valid (*7*), and our trial calculation is consistent with recently published estimates based on direct measurements of phytoplankton photosynthesis under varying $O_3$ thickness in the Antarctic (*36*). Support is also provided by the comparison between our weighting function and other spectra (*7*, *28*, *29*).

Our interpretation of the interaction of UVA and UVB differs from that of Smith *et al.* (*4*): they suggested that UVA played an important role in photoprotection through a mechanism of UVA-induced photoregulation of cell responses to UVB. Thus, UVA was thought to be responsible for the relatively low sensitivity of near-surface phytoplankton to enhanced UVB from $O_3$ depletion. Our analysis suggests that incident UVA in the Antarctic has a net damaging effect and accounts for most inhibition of phytoplankton photosynthesis by UV under all $O_3$ conditions (Fig. 4). Relatively small near-surface responses to UVB are consistent with the predictions of our biological weighting function.

Our analytical model and experimental system are appropriate for measuring and describing the short-term effects of UV radiation on aquatic photosynthesis. These techniques can be used to make direct measurements on natural populations of phytoplankton to assess the natural variability of the weighting function for the inhibition of photosynthesis by UV. The effects of UV on photosynthesis are a function of the duration as well as of the magnitude of exposure (*37*), and phytoplankton can move vertically through the water column at different rates (*6*, *19*, *38*), so the kinetics of photoinhibition and recovery should be incorporated into models of water column photosynthesis (*13*, *37*, *39*). As progress is made toward describing these short-term effects of UV on aquatic photosynthesis, the influence of UV on photoprotective responses (*40*), survival, growth rate (*41*), and species succession of phytoplankton (*42*) should also be considered.

## REFERENCES AND NOTES


1. J. G. Anderson, D. W. Toohey, W. H. Brune, *Science* 251, 39 (1991); M. R. Schoeberl and D. L. Hartmann, *ibid.*, p. 46; R. Stolarski *et al.*, *ibid.* 256, 342 (1992).
2. S. Solomon, *Rev. Geophys.* 26, 131 (1988).
3. D. Lubin, J. E. Frederick, C. R. Booth, T. Lucas, D. Neuschuler, *Geophys. Res. Lett.* 16, 783 (1989); K. Stamnes, J. Slusser, M. Brown, *ibid.* 17, 2181 (1990).
4. R. C. Smith *et al.*, *Science* 255, 952 (1992).
5. R. C. Smith and K. S. Baker, *Photochem. Photobiol.* 29, 311 (1979).
6. *Environmental Effects of Ozone Depletion: 1991 Update* (United Nations Environment Programme, Nairobi, Kenya, 1991); D.-P. Häder and R. C. Worrest, *Photochem. Photobiol.* 53, 717 (1991).
7. R. D. Rundel, *Physiol. Plant.* 58, 360 (1983); M. M. Caldwell, L. B. Camp, C. W. Warner, S. D. Flint, in *Stratospheric Ozone Reduction, Solar Ultraviolet Radiation, and Plant Life*, R. C. Worrest and M. M. Caldwell, Eds. (Springer, Berlin, 1986), pp. 87–111.
8. R. C. Smith, K. S. Baker, O. Holm-Hansen, R. S. Olson, *Photochem. Photobiol.* 31, 585 (1980).
9. T. P. Coohill, *ibid.* 50, 451 (1989).
10. T. Hirosawa and S. Miyachi, *Arch. Microbiol.* 135, 98 (1983); G. Samuelsson, A. Lönneborg, E. Rosenqvist, P. Gustafson, G. Öquist, *Plant Physiol.* 79, 992 (1985); D. H. Greer, J. A. Berry, O. Bjorkman, *Planta* 168, 253 (1986).

11. R. C. Smith and K. S. Baker, *Oceanogr. Mag.* 2, 4 (1989).
12. The formulation is like that presented by T. Platt, C. L. Gallegos, and W. G. Harrison [*J. Mar. Res.* 38, 687 (1980)] and comparable to other models of photoinhibition (*13*). The saturation parameter, $E_s$, is analogous to the adaptation parameter, $I_k$ [J. F. Talling, *New Phytol.* 56, 133 (1957)] and is related to the initial slope of the $P^B$ versus $E_{PAR}$ relation, $\alpha$ (in grams of carbon per gram of chlorophyll per hour per watt per meter squared), by the equation $\alpha = P_s^B/E_s$.
13. P. J. Neale, in *Photoinhibition*, D. J. Kyle, C. B. Osmond, C. J. Arntzen, Eds. (Elsevier, Amsterdam, 1987), p. 35.
14. The algebraic form of the inhibition term is consistent with predictions of a simple kinetic model of photoinhibition of photosynthesis as a balance between damage and recovery (*13*, *15*).
15. M. P. Lesser, J. J. Cullen, P. J. Neale, in preparation.
16. The parameter $\bar{\epsilon}_{PAR}$ is analogous to wavelength-independent inhibition parameters in other models of photosynthesis versus irradiance. In accord with other models of $P^B$ versus $E_{PAR}$ [J. J. Cullen, *Deep-Sea Res.* 37, 667 (1990)], spectral dependency between 400 and 700 nm is not considered here. This refinement [R. R. Bidigare, B. B. Prézelin, R. C. Smith, in *Primary Productivity and Biogeochemical Cycling in the Sea*, P. G. Falkowski and A. Woodhead, Eds. (Plenum, New York, 1992), p. 175] could be incorporated into future models.
17. The biologically weighted dose rate per unit $E_{PAR}$ is given by

$$(1/E_{PAR}) \sum_{\lambda=280\ nm}^{400\ nm} \epsilon(\lambda)E(\lambda)\Delta\lambda$$

The units for the summation are dimensionless. In practice, the effects of UV were analyzed for wavelengths from 286 to 390 nm.
18. K. Richardson, J. Beardall, J. A. Raven, *New Phytol.* 93, 157 (1983); L. W. Harding, Jr., T. R. Fisher, Jr., M. A. Tyler, *Biol. Oceanogr.* 4, 403 (1987).
19. J. J. Cullen and M. R. Lewis, *J. Plankton Res.* 10, 1039 (1988).
20. W. G. Harrison and T. Platt, *Polar Biol.* 5, 153 (1986).
21. Experimental cultures were grown in enriched artificial seawater medium [R. R. L. Guillard and J. H. Ryther, *Can. J. Microbiol.* 8, 229 (1962)]. f/2 for the diatom *Phaeodactylum* sp., f/2 −Si for the dinoflagellate *Prorocentrum micans* (clone PRORO III of the Provasoli-Guillard Culture Collection for Marine Phytoplankton) at 20°C on a 12 hour:12 hour light:dark cycle illuminated by full-spectrum fluorescent lamps at a quantum scalar irradiance of 75 μmol $m^{-2}$ $s^{-1}$, ~16 W $m^{-2}$ (*37*). During growth, UVB was excluded by the walls of the polycarbonate culture vessels. Photosynthesis was estimated as the uptake of $H^{14}CO_3^-$ into organic compounds during 45-min incubations as determined by scintillation counting after acidification of 0.75-ml aliquots [M. R. Lewis and J. C. Smith, *Mar. Ecol. Prog. Ser.* 13, 99 (1983); (*37*)]. Uptake was corrected for time-zero controls.
22. M. R. Lewis, R. E. Warnock, T. Platt, *Limnol. Oceanogr.* 30, 794 (1985).
23. Limitations of the routine radiometric measurements compelled us to restrict analysis to wavelengths from 286 to 390 nm. False signals from stray light (principally below 280 nm) were detected by comparison of spectra with different long-pass filters (*37*) and were ignored. Analysis of irradiance spectra showed that there was no significant transmittance of wavelengths <286 nm in any of the treatments. Having the upper limit at 390 nm rather than at 400 nm has no bearing on the results or conclusions.
24. Principal component analysis [D. F. Morrison, *Multivariate Statistical Methods* (McGraw-Hill, New York, 1976)] was performed on a correlation matrix of UV irradiance measured in each of 209 0.5-nm wave bands (286 to 390 nm) and expressed as $[E(\lambda)\Delta\lambda/E_{PAR}]$. There were 50 to 60 treatment cases in each experiment, and the results of two experiments were combined for each analysis. Each irradiance treatment was normalized to corresponding $E_{PAR}$ followed by calculation of the correlation matrix. This procedure equalized the contribution of each spectrum and each wavelength to the derived components. The SHAZAM program was used to analyze the 209-variable correlation matrix [K. J. White, *Am. Stat.* 41, 80 (1987)], component scores were derived from the principal component eigenvectors, and UV irradiance was expressed as standard normal deviates at each wavelength. Component score variance was scaled to component eigenvalue, that is, the amount of original variable variance accounted for by that component. The overall relation of the component scores to the original UV measurements is thus

$$\frac{[E(\lambda) - \bar{E}(\lambda)]\Delta\lambda}{E_{PAR}} = \sum_{i=1}^{N} c_i \phi_i(\lambda) \cdot SD(\lambda)$$

where $c_i$ is the dimensionless score for each of $N$ components, $\phi_i(\lambda)$ is the dimensionless spectral weighting, and $SD(\lambda)$ is the standard deviation of $E(\lambda)\Delta\lambda/E_{PAR}$. The wavelength-specific amplitude used to obtain $E(\lambda)\Delta\lambda/E_{PAR}$ from mean $E(\lambda)\Delta\lambda/E_{PAR}$ is the product $\phi_i(\lambda)SD(\lambda)$, which is the spectral component loading in Fig. 2C.
25. The first two of $N = 209$ spectral components accounted for >95% of the variance of the treatment UV; that is, the sum of the eigenvalues for the components was >198.
26. Iterative nonlinear regression was used to fit Eq. 1 from experimental data using $E_{inh}' = E_{PAR}(h_0 + h_1c_1 + h_2c_2)$, where $h_0$ is the biological weighting for both $E_{PAR}$ and the mean UV spectrum:

$$h_0 = \bar{\epsilon}_{PAR} + \sum_{\lambda=286\ nm}^{390\ nm} \frac{\epsilon(\lambda)\bar{E}(\lambda)\Delta\lambda}{E_{PAR}}$$

The expression $h_1c_1 + h_2c_2$ is translated to $\Sigma\,\epsilon(\lambda)E(\lambda)\Delta\lambda$, based on the relation between the $c_i$ and $E(\lambda)$ (*24*). The two coefficients of $E(\lambda)$ in the substituted expression were combined to give the statistical estimates of $\epsilon(\lambda)$. The estimated biological weighting function is then used to calculate independently $\Sigma\,\epsilon(\lambda)\bar{E}(\lambda)\Delta\lambda$ so that $\bar{\epsilon}_{PAR}$ can be recovered as

$$\bar{\epsilon}_{PAR} = h_0 - \sum \frac{\epsilon(\lambda)\bar{E}(\lambda)\Delta\lambda}{E_{PAR}}$$

For the experiments here, estimated $\bar{\epsilon}_{PAR}$ could not be statistically distinguished from 0 (*27*), consistent with the result (data not shown) that, over the range of $E_{PAR}$ used here, no photoinhibition was observed when UV was totally excluded (that is, by the 400-nm long-pass filter).
27. Variance estimates for $\epsilon(\lambda)$ and $\bar{\epsilon}_{PAR}$ were calculated from the asymptotic variances and covariances of the final estimates of $h_0$ and $h_i$, and linear error propagation [P. R. Bevington, *Data Reduction and Error Analysis for the Physical Sciences* (McGraw-Hill, New York, 1969), p. 56].
28. D. Lubin *et al.* [*J. Geophys. Res.* 97, 7817 (1992)] describe results of experiments by B. G. Mitchell, [in *Response of Marine Phytoplankton to Natural Variations in UV-B Flux*, B. G. Mitchell, O. Holm-Hansen, I. Sobolev, Eds. (proceedings of a workshop, Scripps Institution of Oceanography, La Jolla, CA, 5 April 1990; available from Chemical Manufacturers Association, Washington, DC, 1990)]. A recently published weighting function (*29*) is similar, except that the slope between 300 and 325 nm is less steep, nearly the same as our weighting function (Fig. 3C).
29. E. W. Helbling, V. Villafañe, M. Ferrario, O. Holm-Hansen, *Mar. Ecol. Prog. Ser.* 80, 89 (1992).
30. L. W. Jones and B. Kok, *Plant Physiol.* 41, 1037 (1966).
31. R. B. Setlow, *Proc. Natl. Acad. Sci. U.S.A.* 71, 3363 (1974).
32. H. Maske, *J. Plankton Res.* 6, 351 (1984); B. Bühlmann, P. Bossard, U. Uehlinger, *ibid.* 9, 935 (1987).
33. P. J. Neale, J. J. Cullen, M. P. Lesser, in preparation.
34. Data from the National Science Foundation Division of Polar Programs UV monitoring station at Arrival Heights, McMurdo, Antarctica, were provided by C. R. Booth (personal communication). Integral irradiance measured for 400 to 600 nm was multiplied by 1.44 to estimate integral irradiance from 400 to 700 nm. Because $E_{PAR}$ was different on the two dates, proportionality factors were applied to $E(\lambda)$ to obtain estimates at $E_{PAR}$ = 200 W $m^{-2}$, from original $E_{PAR}$ values of 157 W $m^{-2}$ (28 October 1990) and 257 W $m^{-2}$ (10 November 1990).
35. The relative change in photosynthesis is calculated for $E_{PAR} >> E_s$ so that changes depend only on $E_{inh}'$. We estimated standard errors for the relative change as previously described (*27*), assuming fixed spectral irradiance; they ranged from 1 to 2% (88 df).
36. Our prediction of a dominant influence of UVA is consistent with that of earlier workers (*4*, *28*, *29*, *32*), and our estimate of the incremental influence of $O_3$ depletion on photosynthesis is roughly consistent with that of Smith *et al.* (*4*). However, Smith *et al.* measured near-surface photoinhibition of 60 to 70% associated with UVA substantially higher than our prediction. The difference may be due to time scale or species dependence. Our time scale was 45 min, whereas theirs was 7 to 10 hours.
37. J. J. Cullen and M. P. Lesser, *Mar. Biol.* 111, 183 (1991).
38. K. L. Denman and A. E. Gargett, *Limnol. Oceanogr.* 28, 801 (1983).
39. C. Pahl-Wostl and D. M. Imboden, *J. Plankton Res.* 12, 1207 (1990); G. S. Janowitz and D. Kamykowski, *ibid.* 13, 983 (1991).
40. C. S. Yentsch and C. M. Yentsch, in *The Role of Solar Ultraviolet Radiation in Marine Ecosystems*, J. Calkins, Ed. (Plenum, New York, 1982), pp. 691–700; D. Karentz, F. S. McKuen, M. C. Land, W. C. Dunlap, *Mar. Biol.* 108, 157 (1991).
41. J. Calkins and T. Thordardottir, *Nature* 283, 563 (1980); P. L. Jokiel and R. H. York, Jr., *Limnol. Oceanogr.* 29, 192 (1984); D. Karentz, J. E. Cleaver, D. L. Mitchell, *J. Phycol.* 27, 326 (1991).
42. R. C. Worrest, B. E. Thomson, H. V. Dyke, *Photochem. Photobiol.* 33, 861 (1981).
43. Spectral irradiance was measured with a calibrated diode-array spectroradiometer including a quartz fiber-optic probe (*37*). A quantum scalar irradiance meter (Biospherical Instruments QSL-100 with a special small $4\pi$ collector) was used to measure PAR (in micromoles per square meter per second), which was converted to $E_{PAR}$ with reference to measured spectral irradiance from 400 to 700 nm. Irradiance scans from 350 to 750 nm were used to determine characteristic ratios of $E(390\ nm):E_{PAR}$ for each of the eight spectral treatments. The UV spectral irradiance in each treatment was calculated as the product of the quantum irradiance–based estimate of $E_{PAR}$ (which was measured most frequently), the characteristic $E(390\ nm):E_{PAR}$ ratio for the WG-series spectral treatment, and $E(\lambda)/E(390\ nm)$ from a 275- to 400-nm UV spectrum for each irradiance treatment (Fig. 2A).
44. Supported by the National Science Foundation Department of Polar Programs (grants DPP 881768 and DPP 9018441), the National Aeronautics and Space Administration (grant NAGW 2072), the Office of Naval Research (grant N00014-92-J-1099), and the Natural Sciences and Engineering Research Council of Canada. We thank W. K. Bellows for technical assistance, and W. F. Vincent, M. R. Lewis, and T. L. Richardson for comments. Bigelow Laboratory contribution 92003.

19 May 1992; accepted 30 July 1992